Lipid Droplet-Specific Red Aggregation-induced Emission Luminogens: Fast Light-up of Gram-positive pathogens for Identification of Bacteria

Xiaohui Wang,[a#] Meirong Song,[d#] Yiwei Liu,[a] Xing Feng,*[a] Carl Redshaw,[e] Dong Wang,[c] Kui Zhu,[d] Ying Li,*[bc] Ben Zhong Tang*[cf]

[a] Guangdong Provincial Key Laboratory of Information Photonics Technology. School of Material and Energy, Guangdong University of Technology, Guangzhou 510006, P. R. China. E-mail: hyxhn@sina.com

[b] Guangzhou Municipal and Guangdong Provincial Key Laboratory of Molecular Target & Clinical Pharmacology, the NMPA and State Key Laboratory of Respiratory Disease, School of Pharmaceutical Sciences and the Fifth Affiliated Hospital, Guangzhou Medical University, Guangzhou 511436, China. E-mail: liying5797@126.com

[c] Center for AIE Research, College of Materials Science and Engineering, Shenzhen University, Shenzhen 518060, China

[d] National Center for Veterinary Drug Safety Evaluation, College of Veterinary Medicine, China Agricultural University, Beijing, China, No. 2 Yuanmingyuan West Rd, Beijing 100193, China

[e] Department of Chemistry, University of Hull, Cottingham Road, Hull, Yorkshire HU6, UK

[f] Shenzhen Institute of Molecular Aggregate Science and Engineering, School of Science and Engineering, The Chinese University of Hong Kong, Shenzhen 518172, China mail: tangbenz@cuhk.edu.cn

KEYWORDS aggregation-induced emission, red emitter, bacterial staining, Gram-positive pathogens, imaging mechanism.

ABSTRACT: Gram-positive (G+) and Gram-negative (G-) bacteria require considerable difference in their therapeutic strategies. Thus, the development of highly efficient techniques for differentiating G+ and G- bacteria is of vital importance for practical clinical applications. Herein, we present 2-((10-ethyl-10H-phenothiazin-3-yl)methylene)-1H-indene-1,3(2H)-dione(PH-ID), an electrically neutral, red fluorophore with aggregation-induced enhanced emission (AIEE) characteristic, to selectively stain G+ bacteria membrane with high specificity and sensitivity. The staining result can be accomplished within 10 min and can be read by the naked eye. Lipopolysaccharide (LPS) in the outer leaflet of the membrane of G- bacteria prevents the staining of the bacteria by PH-ID, which is the mechanism underlying the Gram selectivity of PH-ID. This study not only provides a highly efficient method for bacteria imaging and discrimination, but also provides insight into the bacteria imaging mechanism, which is beneficial for the exploration of new electroneutral AIE luminogens for bacteria surveillance applications.

The evolution of humanity is the story of mutual creation and destruction between humans and microbes, and the presence of pathogenic bacteria would seriously endanger human health and life.[1] The use of antibiotics, such as penicillin,[2] plays a significant role in fighting against pathogenic bacteria. However, the abuse of antibiotics accelerates the evolution of bacteria, leading to the emergence of multidrug resistant (MDR) 'superbugs'.[3] Given that Gram-positive (G+)/ Gram-negative (G-) bacteria cause diseases *via* different mechanism, it is key to determine the type of bacteria in various fields including clinical administration, the ecosystem, as well as in the food industry.[4] The G+ bacteria, such as *Staphylococcus aureus* (*S. aureus*), methicillin-resistant *Staphylococcus aureus* (MRSA) are common types of nosocomial pathogens and contribute to community infection.[5] In general, G+ bacteria have a thick peptide polysaccharide layer (about 20-80 nm), but no external lipid membrane. In contrast, G- bacteria have a thinner peptide polysaccharide layer with an external lipid membrane.[6] Thus, based on the difference between their outer wall structures, the traditional Gram-staining method can be used to differentiate between the G+/G- bacteria, but it is worth noting that this method still has accuracy and efficiency challenges, as well as issues of sensitivity of colorimetry.[7]

Fluorescence imaging is one of the most important and preferred tools by which to track ubiquitous pathogens vividly, due to its advantages of visualization, high sensitivity, super-resolution, fast response, and non-invasiveness.[8,9] A key point of fluorescence imaging is to develop novel fluorescence materials for identifying bacteria *via* fast and specifical light-up Gram-staining.[7] Conventional fluorescence dyes, such as rhodamine, BODIPY and cumarin, prefer to undergo an aggregation-caused quenching (ACQ) phenomenon, and exhibit strong emission in diluted solution. However, the fluorescence would be quenched upon aggregate formation or an increase of concentration.[10] In addition, conventional fluorescence dyes are susceptible to photobleaching under laser excitation, leading to short operating cycles.[11,12]

In contrast, aggregation-induced emission luminogens (AIEgens) [13] emit bright fluorescence with good photostability at high concentration or in the aggregated state, showing a quite different fluorescent property compared to conventional dyes.[14] In particular, red emitters with the AIE characteristic exhibit unique advantages compared with traditional fluorescence dyes. These advantages include: (1) high signal-to-noise ratio, (2) low biological background interference, (3) considerable penetration depth, (4) good photostability, and (5) long-term *in situ* imaging.[15,16] Up to

This document is the Accepted Manuscript version of a Published Work that appeared in final form in ACS Materials Letters, copyright © American Chemical Society after peer review and technical editing by the publisher. To access the final edited and published work see 10.10.1021/acsmaterialslett.2c00551

now, various AIEgens with red emission have been exploited for identifying the cellular organelles, visualizing proliferation/apoptosis of cells *in vitro*,[17] and for the diagnosis and treatment of tumors,[18] as well as for the real-time monitoring of bacterial infection.[19,20] However, the use of (red) AIE fluorescence probes for living bacterial differentiation remains rare.[21,22] Since our group reported that the AIEgen can be used for differentiating dead and living bacteria in 2014,[23] many new AIE-based fluorescent probes have been explored for the discrimination and killing of ubiquitous pathogens (including G+ and G- bacteria). [24] We previously reported a microenvironment-sensitive AIEgen to discriminate three pathogens (G+ bacteria, G- bacteria and fungus) simultaneously *via* the naked-eye, where the AIEgen can specifically locate at different sites of three kinds of pathogens and this leads to tunable color emission.[25] This is an efficient approach for the rapid and qualitative identification of pathogen types, but such a system does not operate in a quantitative fashion.[25] Generally, it is widely reported that various cationic AIEgens can act as bacteria staining or screening agents and some probes have shown potential for inactivating both G+/ G- bacteria *via* a photoinduced process.[26,27,28] By comparison, the anionic or neutral AIEgens have insufficient activity to photosensitize the G+ bacteria. Liu *et al*. reported a neutral, light-up red fluorescent probe bearing a vancomycin unit with AIE characteristics for the selective imaging and photodynamic destruction of G+ bacteria. Our group has reported a neutral simple green-light emitter with AIE feature, which was used for differentiating the G+ bacteria from G- bacteria and fungus with excellent selectivity.[29] However, neutral probes that can distinguish bacteria are rarely reported and are a challenge to development.

In this study, we have developed a phenothiazine-based AIE electrically neutral fluorophore PH-ID (Scheme 1), which was inspired by the high resolution and selectivity of phenothiazine derivatives to lipid droplets (LDs).[30] PH-ID has superior specificity for staining LDs with high photostability. Interestingly, we found that PH-ID can selectively bind to the membrane of G+ bacteria and hardly stains G- bacteria. Further studies indicated that the LPS of the outer membrane (OM) was the obstacle for staining G- bacteria with PH-ID (Scheme 1). These fundings shed light on the development of the next generation of AIEgens for distinguishing between G- and G+ bacteria.

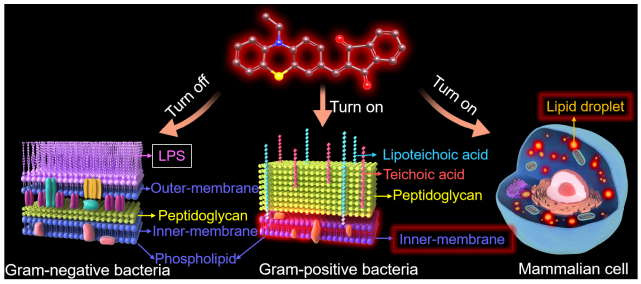

Scheme 1. Working mechanism of PH-ID to selectively light up G+ bacteria and lipid droplets of mammalian cells.

Synthesis and Characterization: The compound PH-ID was synthesized following previous reports.[30] Using phenothiazine as a starting material, an alkylation and formylation reaction was conducted with good yield, and this was followed by the high yield Knoevenagel condensation of aldehyde phenothiazine with 1,3-indanedione (**Scheme** S1). $^{1}H/^{13}C$ NMR and high-resolution mass spectra (HRMS) were performed to identify the molecular structure and purity. The indanedione and phenothiazine units act as strong electron withdrawing and donating groups, respectively. The optimized molecular geometry of PH-ID was investigated using the DFT/B3LYP method at a 6-311G (d,p) set basis. As shown in Figure 1, the compound PH-ID contains a phenothiazine and indanedione unit, which are coplanar with each other, and this results in a short intramolecular hydrogen bond (H-bond) with a distance of 2.06 Å. Moreover, the highest occupied molecular orbital (HOMO) energy level was almost located on the phenothiazine unit and the lowest unoccupied molecular orbital (LUMO) energy level was not only spread over the indanedione units, but also over part of the phenothiazine ring, respectively. The pull-push structure of PH-ID with separated HOMO and LUMO levels can contribute to the intramolecular charge transfer (ICT) process, and may lead to a large red-shifted emission.

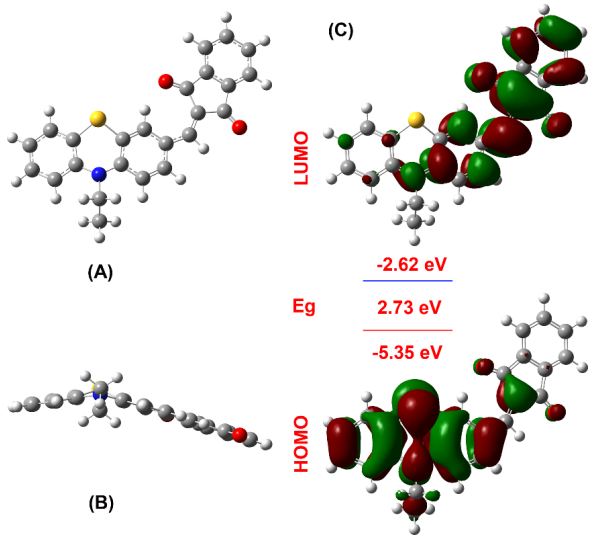

Figure 1. The optimized molecular structure of the phenothiazine-based compound, (A) top view, (B) side view, (C) the HOMOs/LUMOs of PH-ID calculated by B3LYP/6-311G*.

Photophysical Properties: UV-vis absorption and fluorescence spectra of PH-ID in THF (10 μM) were measured, which exhibited maximum absorption and emission band at 496 nm and 691 nm, respectively. The large Stokes shift (195 nm) of PH-ID makes it an ideal candidate as a fluorescent probe due to the minimization of the self-quenching fluorescence effect (**Figure 2**A). In addition, as the solvent polarity increases from the non-polar solvent hexane to the highly polar dimethyl sulfoxide (DMSO), the maximum emission peak red-shifted from 623 nm to 735 nm, suggesting that this compound underwent a strong ICT effect (**Figure S**8).

The AIE behavior of PH-ID was examined in DMSO with different fractions of added water *via* fluorescence spectral experiments (λ_{ex} = 506 nm). The maximum emission peak was

731 nm in pure DMSO, and when the water fraction (f_w) increased from 0% to 50%, the emission intensity decreased about 5-fold. Afterwards, the emission gradually enhanced as f_w increased to over 50%, with a slightly blue-shifted emission to 721 nm. When f_w increased to 80%, the compound displayed dual emission with a maximum emission ($\lambda_{max\,em}$) at 721 nm and a shoulder peak at 773 nm. The emission intensity of the latter further increased when f_w increased to 99%. Moreover, the fluorescence lifetime was investigated in order to understand the electronic transition of dual emission. The fluorescence lifetime slightly increased from 1.009 ns at $\lambda_{max\,em}$ = 731 nm) in DMSO to 1.354 nm at $\lambda_{max\,em}$ = 721 nm) and 1.345 nm at $\lambda_{max\,em}$ = 773 nm in f_w = 99%, indicating that the long-wavelength emission at 731 nm is not originating from excimer emission, but maybe that the dipole moment changes upon excitation from the ground state to the excited state in the aggregated state, resulting in a charge-transfer emission. [31] The quantum yield (Φ_f) of PH-ID was 0.06 in THF and 0.11 in the solid state respectively, indicating that PH-ID exhibited brighter emission in the solid state, which is a typical AIE feature. Furthermore, the radiative decay rate (K_r) and nonradiative decay rate (K_{nr}) of PH-ID were calculated by the equations $K_r = (\Phi/\tau)$ and $K_{nr} = 1/\tau - k_r$, respectively. As shown in Table S1, the k_r value slightly decreased from 3.17 ×10^7 S^{-1} in THF to 2.69 ×10^7 S^{-1} in the solid state, while the K_{nr} decreased from 49.7 ×10^7 S^{-1} to 21.7 ×10^7 S^{-1}, which indicated that any energy loss *via* a non-radiation transition has effectively been blocked, resulting in emission enhancement during the radiation process in the solid state. Thus, compound PH-ID was confirmed to be a material with AIE activity (Figures 2B-2D).

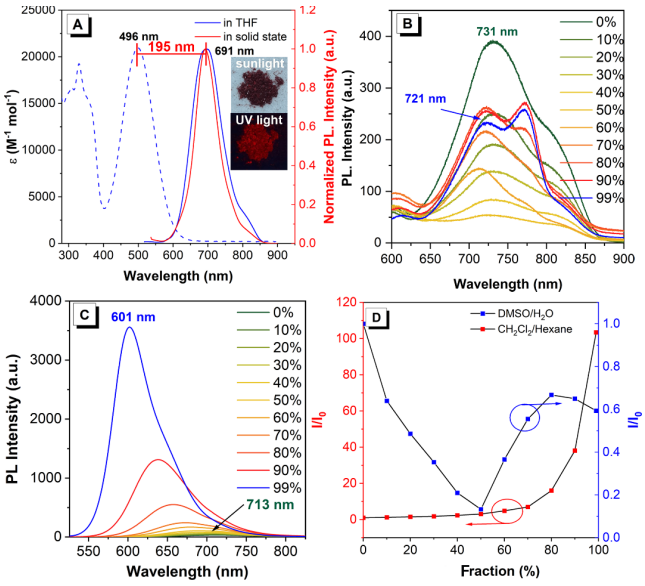

Figure 2. (A) UV-vis and fluorescence spectra of PH-ID in THF and in the solid-state. The fluorescence spectra in (B) DMSO/water mixtures with different water fractions (f_w) and (C) DCM/hexane mixtures with different hexane fractions, (D) Plots of relative PL intensity (I/I_0) *versus* the composition of DMSO/water mixtures (blue line), and DCM/hexane mixtures (red line), where I_0 is the PL intensity in pure THF. Insert: photograph of PH-ID under sunlight and UV light (λ_{ex} = 365 nm) with red emission.

To further examine the influence of solvent polarity on the AIE effect of PH-ID, the fluorescence spectra were measured in a dichloromethane/hexane (DCM/hexane) system with different hexane fractions (f_H). As shown in Figure 2C, PH-ID emitted weak red fluorescence with a maximum emission peak at 713 nm in DCM. The solution polarity decreased as hexane was added into the system, and the PL intensity gradually enhanced by *ca*. 100-fold with a blue shift from 713 nm (f_H = 0%) to 601 nm (f_H = 99%). This can be ascribed to the ICT effect would be counteracted as the non-polar hexane was added, and then the AIE effect overwhelms the ICT effect. Such results further confirmed that PH-ID was AIEE-active and such emission behavior was normal and frequently took place in AIE-active luminogens with donor-acceptor systems.[32]

Cellular Imaging, Photostability and Cytotoxicity: The red emitter PH-ID displayed a large Stokes shift and a considerable quantum yield in the aggregate state, which made it an ideal fluorescent probe for bioimaging applications. As illustrated in Figure 3A, bright red fluorescence within COS7 and HeLa cells can be observed after incubation with PH-ID for 10 min at 37°C. To verify the specificity of the PH-ID for cell imaging, co-localization experiments were carried out by incubating COS7 and HeLa cells with PH-ID followed by BODIPY staining. The latter is a commercial probe for specific lipid drops (LDs) staining. The results indicated that PH-ID can selectively stain the LDs by co-localization with BODIPY, with a high overlap coefficient of 0.933 and 0.937 for the COS7 and HeLa cells, respectively, which indicated the superior specificity of PH-ID for staining LDs. The results are consistent with previous reports,[30,33] and reveals that molecules containing the indanedione unit are excellent fluorescent probes for LDs imaging.

The high lipophilicity associated with fluorescence dyes is due to either high hydrophobicity or high calculated logP (ClogP: *n*-octanol/water partition coefficient) values, while ClogP values of ideal lipophilic organic dyes are larger than 5.[34] The lipophilicity of the PH-ID was evaluated with a ClogP value of 5.50 by using ChemBioDraw 14.0, which was higher than the commercial lipophilic dye BODIPY (5.03).[35,36] Thus, PH-ID is an ideal biosensor for LDs imaging with high specificity and sensitivity.

Photostability is one of the key parameters for evaluating the advantages of fluorescent bioprobes. Under continuous laser excitation and sequential scanning with a confocal laser scanning microscope (CLSM), the fluorescence signals of PH-ID slightly decreased to 93% compared to its initial values after 100 scans (Figure 3C), whilst the morphology of the cells was still very clear after 100 scans (Figure 3B). In comparison, the fluorescence signals of BODIPY faded to 88% under the same conditions (Figure 3C). Thus, PH-ID is favorable for long-term imaging.

Inherent biocompatibility is a prerequisite for potential application in bioimaging. The 3-(4,5-dimethyl-2-thiazolyl)-2,5-diphenyl-2-H-tetrazolium bromide (MTT) assay was used to evaluate the cytotoxicity of different concentrations of PH-ID incubated with human umbilical vein endothelial cells (HUVECs), NIH-3T3, COS7, human hepatocytes LO2, HeLa and 4T1 cells over 24 h. More than 95% of the cells were alive for 24 h even at a concentration of up to

20 μM (Figure S10). In addition, the cytotoxicity of PH-ID was further evaluated using a Calcein AM/prodium iodide (PI) assay. As shown in Figure S11, the HeLa cells exhibited green fluorescence at various concentrations of PH-ID from 0 to 20 μM. The HeLa cells were distributed in radial or swirl patterns covering the plate surface and displayed normal cellular morphology, without the appearance of dead cells. These results indicated the favorable biocompatibility of PH-ID.

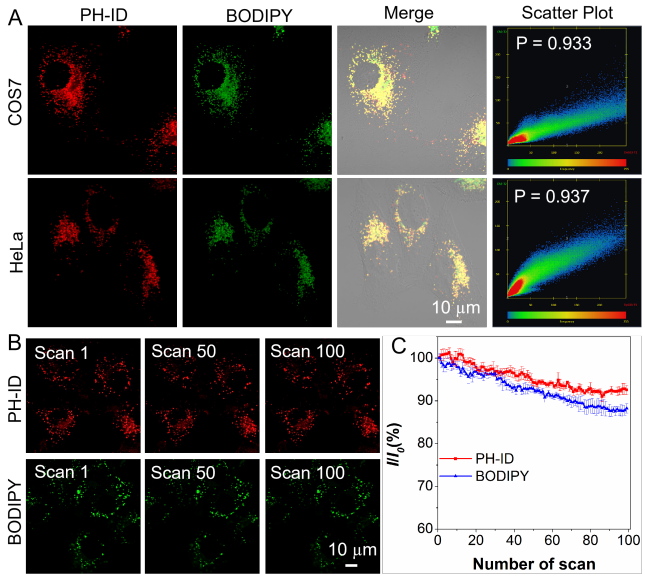

Figure 3. (A) Co-localization of PH-ID and BODIPY in COS7 and HeLa cells. The cells were stained with PH-ID (10 μM) for 10 min, followed by the staining with BODIPY (1 μM) for 15 min. A scatter plot indicates a correction coefficient between PH-ID and BODIPY. (B) Fluorescence imaging of COS7 cells with increasing number of scans to test the photostability of PH-ID (10 μM) and BODIPY (1 μM) in COS7 cells under continuous laser irradiation. (C) I/I_0 (%) of PH-ID and BODIPY in COS7 cells with increasing number of scan. PH-ID: λ_{ex} = 488 nm, λ_{em} = 600-700 nm; BODIPY: λ_{ex} = 488 nm, λ_{em} = 500-530 nm.

Bacteria Staining and Imaging: Given that the PH-ID with high photostability and biocompatibility can realize LD imaging with high specificity, how about its capability for bacteria staining? To investigate this, four species of G+ bacteria (*Staphylococcus epidermidis* (*S. epidermidis*), *Staphylococcus aureus* (*S. aureus*), MRSA, vancomycin-resistant *Enterococcus* (VRE)) and six species of G- bacteria (*Escherichia coli* (*E.coli*), *E.coli* ToP10, multidrug resistant *E.coli* (MDR *E. coli*) and *Klebsier pneumonia* (*K. pneumonia*) ATCC43816, *K. pneumoniae* ATCC43816 *Δ Waac*, MDR *K. pneumoniae*) were selected for testing the bacteria staining and imaging using PH-ID as the fluorescent probe. As shown in Figure 4 and Figures S12-S14, the fluorescence imaging showed that PH-ID (5 μM, 10 min) can selectively light-up the G+ bacteria, including *S. epidermidis*, *S. aureus*, MRSA, and VRE. By contrast, the G- bacteria (such as *E.coli*, *E. coli* Top10, MDR *E.coli*, and MDR *K. pneumoniae*) cannot be stained even at high concentrations of PH-ID (0~25 μM) or under extended incubation time (10~60 min) (Figure S12). These results implied that the PH-ID can selectively combine with the G+ bacteria but not G- bacteria. This may be ascribed to the different structure of the extra outer membrane of the G+ and G- bacteria.[37]

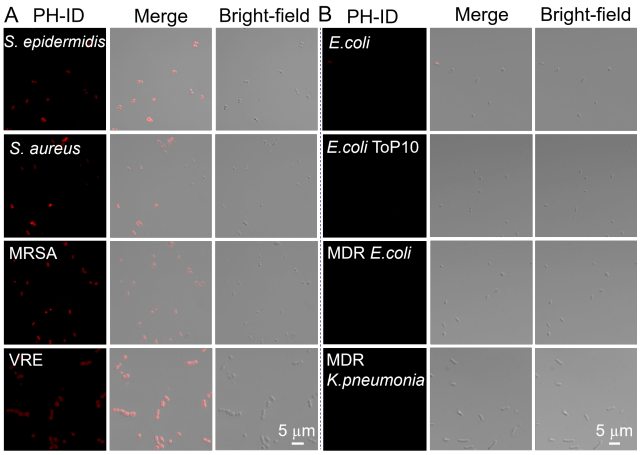

Figure 4. (A) Confocal fluorescence imaging of G+ bacteria (*S. epidermidis*, *S. aureus,* MRSA and VRE) incubated with PH-ID (5 μM) for 10 min. (B) Confocal fluorescence imaging of G- bacteria (*E.coli*, *E.coli* ToP10, MDR *E.coli* and MDR *K. pneumonia*) incubated with PH-ID (5 μM) for 10 min. λ_{ex} = 488 nm, λ_{em} = 600-700 nm.

Generally, viability staining with SYTO9 and propidum iodide (PI) is a frequently used tool in microbiological studies.[38] SYTO9 can stain both dead and live bacteria while PI only stains dead bacteria. In our case, both PH-ID and SYTO9 can stain the *S. aureus* (G+ bacteria) very well with different emission colors. *S. aureus* stained by SYTO9 emitted green fluorescence in the imaging field, while *S. aureus* stained by PH-ID displayed red fluorescence., Some bacteria showed weak green light (SYTO9), while PH-ID has bright fluorescence (Figure S15). The results indicated that PH-ID can better calculate the total fluorescence intensity of certain bacteria. We further characterized the fluorescence of pure bacteria or bacteria/ PH-ID (*S. epidermidis*, *S. aureus,* MRSA and VRE) in DMSO/phosphate buffer saline (PBS) after incubation with PH-ID (5 μM) for 10 min. As shown in Figure 5, without PH-ID, the G+ bacteria displayed a weak blue emission. On binding of PH-ID to the various G+ bacteria, the emission of all mixtures lightened-up with strong red fluorescence under 365 nm UV irradiation, and the emission intensity was enhanced by 16-fold for *S. epidermidis*, 28-fold for *S. aureus,* 32-fold for MRSA and 35-fold for VRE, respectively. Thus, PH-ID can quickly stain and light-up the G+ bacteria and discriminate bacteria by the naked-eye.

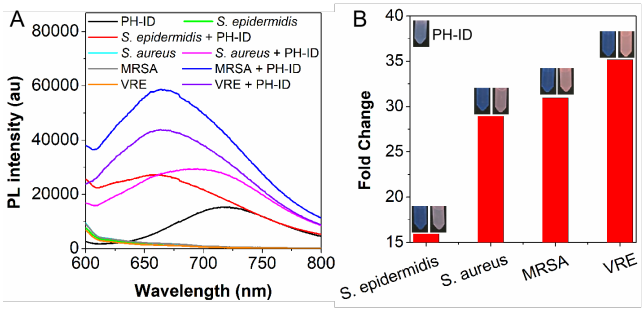

Figure 5. (A) PL spectra of bacteria (10^9 CFU mL^{-1}) with/without PH-ID (5 μM). (B) Fluorescence intensity

change after the bacteria were incubated with PH-ID. Inset: photographs of bacteria and PH-ID/bacteria mixture taken under 365 nm UV irradiation.

Furthermore, the toxicity of PH-ID to bacteria was investigated using the plate counting method. Living S. *epidermidis*, *S. aureus,* MRSA and VRE with a density of 10^8 colony forming units (CFUs mL^{-1}) were incubated with different concentrations of PH-ID for 30 min before their growth on an agar plate. After the bacteria were treated with PH-ID at a high concentration of 20 μM for 30 min, ~99% of the bacteria were still alive (Figures S16-S17). The results indicated that PH-ID is highly biocompatible for fluorescent labeling of G+ bacteria. In addition, some AIEgen molecules can effectively generate reactive oxygen species (ROS) under light irradiation for photodynamic therapy (PDT), against bacteria.[39, 40] We subsequently tested ROS generation by using 2′,7′-Dichlorodihy- drofluorescein diacetate (DCFH-DA), a commercially available ROS indicator. [41]As shown in Figure S18, DCFH and PH-ID showed negligible emission compared with the commercial photosensitizers Ce6 and rose bengal (RB). These results suggest that the PH-ID is a stable biomarker for bacteria imaging.

Mechanism of Mammalian Cells and G+ Bacteria Staining: To gain insight into the staining mechanism of PH-ID with G+ bacteria, *S. aureus* and VRE were selected as G+ bacteria models to co-label bacterial membrane using PH-ID and the commercial membrane-specific dye FM4-64FX.[31] As shown in Figure 6A, PH-ID mainly bound to the bacterial membrane, which almost overlapped with the FM4-64FX with overlap coefficient of P = 0.988 for *S. aureus* and P = 0.975 for VRE, suggesting that the electroneutral red AIEgen PH-ID can specifically bind to the bacterial membrane.

To gain insight into the potential target of PH-ID in the bacterial membrane and the mammalian cell, a microscale thermophoresis (MST) assay was performed to investigate the binding affinity of PH-ID to three major membrane phospholipids of bacteria, including phosphatidylglycerol (PG), phosphatidylethanolamine (PE) and cardiolipin (CL, also known as diphosphatidylglycerol), and one major component phospholipids phosphatidylcholine (PC) of the mammalian cell membrane. [42,43] The main components of cytoplasmic membrane are phospholipids with a hydrophilic head group and two hydrophobic fatty acid chains.[44] The hydrophilic head group determined the charge of phospholipids. For example, PG and CL is anionic, PE is cationic and PC is neutral. Thus, both the hydrophobicity and charge of AIEgens have been considered as the prerequisite for targeting the cell membrane.[45-47] The titration experiments were performed, as different concentration (from 10^{-7} M to 10^{-3} M) of the phospholipid, which was added into the PH-ID (10 μM) solution. The value gradually decreased and the relationship between Δ Fnorm (‰) and lipid concentration is presented in Figure 6B. The equilibrium dissociation constants (KD) between PH-ID and PG, PE, CL and PC were calculated. The results indicated that the PH-ID shows high affinity to phospholipids in both mammalian and bacterial membranes including PG, PE, CL and PC with a robust equilibrium dissociation constant (KD) of 25.8, 25.0, 16.6 and 16.1 μM, respectively. Thus, PH-ID can stain both mammalian cells and bacteria by binding to their membrane components.

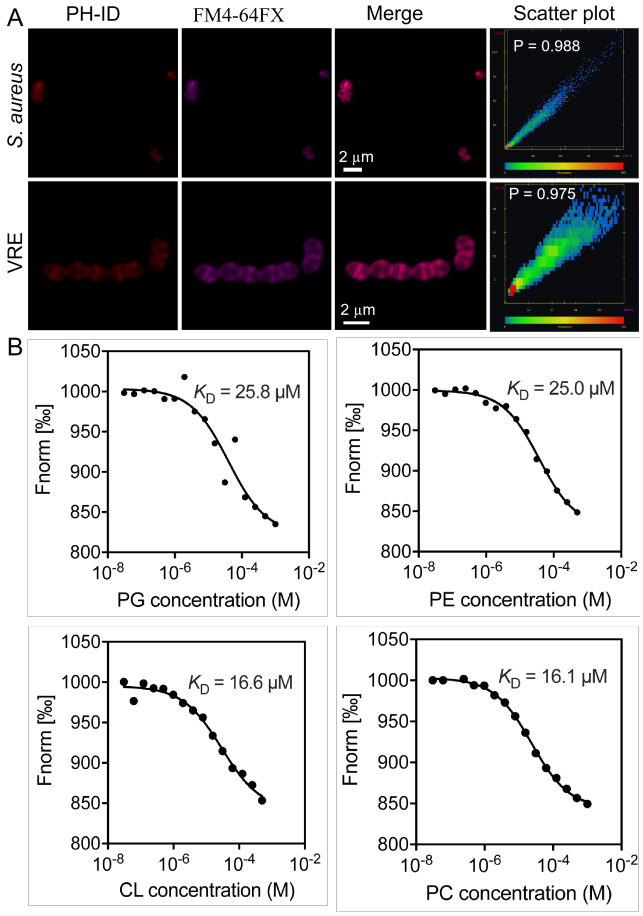

Figure 6. (A) Fluorescence imaging of S. aureus and VRE incubated with PH-ID (5 μM) and FM4-64FX (5 μg mL-1) for 10 min. λex = 488 nm, λem = 600-650 nm; FM4-64FX: λex = 561 nm, λem = 650-700 nm. (B) MST analysis of the interaction between PH-ID and PG, PE, CL and PC.

PE, PG and CL are the main phospholipids in G- bacteria while PG and CL are the main components in most of the G+ bacteria.[48] In this work, PH-ID shows considerable affinity to different phospholipids including PE, PG, and CL (Figure 6B), whether with a charged hydrophilic head group or not. The results suggest that hydrophobicity may be the main factor in order for PH-ID to bind with the membrane. In theory, PH-ID could also bind with the cytoplasmic membrane of G- bacteria. However, PH-ID can hardly stain the G- bacteria. The main difference between Gram- bacteria and G+ bacteria is the OM in G- bacteria, which is an asymmetric lipid bilayer with LPS molecules in the outer leaflet and phospholipids in the inner leaflet.[49] To further explore the role of OM, we tested the label effect of PH-ID on OM deficient *A. baumannii* constructed as reported previously.[50] PH-ID lit-up almost all the *A. baumannii* LPS deficient bacteria, whether at low or high concentration. By contrast, few normal *A. baumannii* were stained by PH-ID even at high concentration (25 μM) over 60 min (Figure 7). These results indicated that the OM is the obstacle to the staining of G- bacteria for PH-ID.

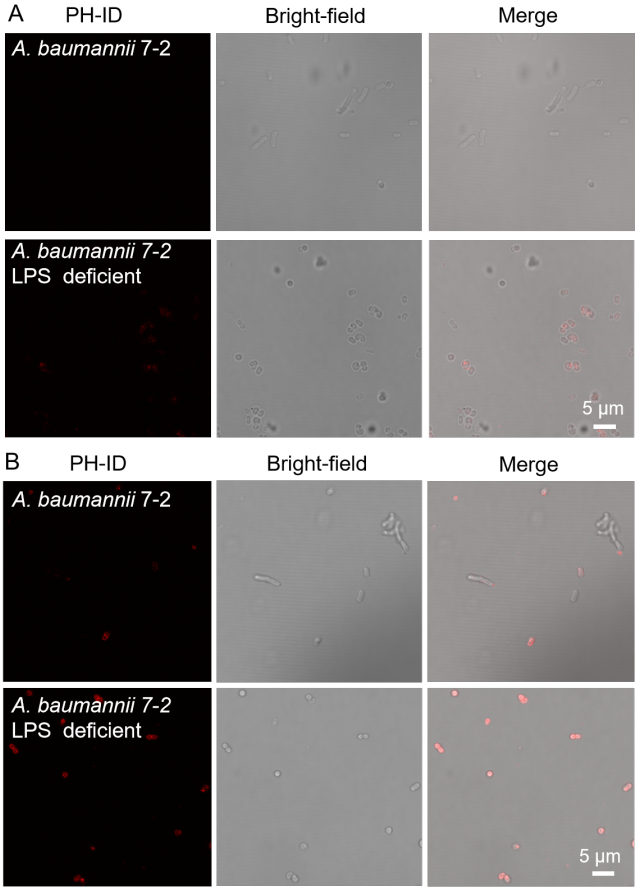

Figure 7. Confocal fluorescence imaging of *A. baumannii* 7-2 and *A. baumannii* 7-2 LPS deficient incubated with 5 μM (A) and 25 μM (B) of PH-ID for 60 min.

In summary, we present an electroneutral red emitter PH-ID with an aggregation-induced emission feature which performed as a highly efficient biological fluorescent probe. Due to the presence of the indanedione unit, PH-ID exhibited good biocompatibility and photostability for the highly selective imaging of lipid droplets in mammalian cells. Moreover, 10 representative bacteria, including four G+ bacteria (*S. epidermidis*, *S. aureus*, MRSA, VRE) and six G- bacteria (*E.coli*, *E.coli* ToP10, MDR *E. coli* and *K. pneumonia* ATCC43816, *K. pneumoniae* ATCC43816 *ΔWaac* and MDR *K. pneumonia*) were selected for investigating the bacteria imaging and Gram-discrimination ability of PH-ID. The results indicated that the G+ bacteria can be rapidly stained (within 10 min) by PH-ID with high specificity, which exhibit bright red emission and can be identified by the naked eye. The staining mechanism study revealed that LPS on the outer membrane of G- bacteria prevents the binding of PH-ID to G- bacteria. Our current work not only provides an electroneutral, lipid droplet-specific, red emitter PH-ID for highly efficient bacteria imaging and discrimination, but also offers new insights for understanding the staining mechanism of bacteria. These results are beneficial for the design of new AIE molecules for staining mammalian cells and bacteria.

ASSOCIATED CONTENT

Supporting Information

The Supporting Information is available free of charge on the ACS Publications website.
Detail experimental procedures, NMR and mass spectra, spectral data and bacterial imaging (PDF)

AUTHOR INFORMATION

Corresponding Author

Xing Feng- Guangdong Provincial Key Laboratory of Information Photonics Technology, School of Material and Energy, Guangdong University of Technology, Guangzhou 510006, P. R. China. Email: hyxhn@sina.com
Ying Li- Guangzhou Municipal and Guangdong Provincial Key Laboratory of Molecular Target & Clinical Pharmacology, the NMPA and State Key Laboratory of Respiratory Disease, School of Pharmaceutical Sciences and the Fifth Affiliated Hospital, Guangzhou Medical University, Guangzhou 511436, China, Center for AIE Research, College of Materials Science and Engineering, Shenzhen University, Shenzhen 518060, China. E-mail: liying5797@126.com
Ben Zhong Tang- Shenzhen Institute of Molecular Aggregate Science and Engineering, School of Science and Engineering, The Chinese University of Hong Kong, Shenzhen 518172, China. Center for AIE Research, College of Materials Science and Engineering, Shenzhen University, Shenzhen 518060, China. mail: tangbenz@cuhk.edu.cn

Author

Xiaohui Wang- Guangdong Provincial Key Laboratory of Information Photonics Technology, School of Material and Energy, Guangdong University of Technology, Guangzhou 510006, P. R. China.
Meirong Song- National Center for Veterinary Drug Safety Evaluation, College of Veterinary Medicine, China Agricultural University, Beijing, China, No. 2 Yuanmingyuan West Rd, Beijing 100193, China
Yiwei Liu- Guangdong Provincial Key Laboratory of Information Photonics Technology, School of Material and Energy, Guangdong University of Technology, Guangzhou 510006, P. R. China.
Dong Wang- Center for AIE Research, College of Materials Science and Engineering, Shenzhen University, Shenzhen 518060, China
Carl Redshaw- Department of Chemistry, University of Hull, Cottingham Road, Hull, Yorkshire HU6, UK
Kui Zhu- National Center for Veterinary Drug Safety Evaluation, College of Veterinary Medicine, China Agricultural University, Beijing, China, No. 2 Yuanmingyuan West Rd, Beijing 100193, China

Author Contributions

X. Wang and M. Song contributed equally.

Notes

Any additional relevant notes should be placed here.

ACKNOWLEDGMENT

This work was supported by the National Natural Science Foundation of China (21975054, 22005195), Natural Science Foundation of Guangdong Province of China (2019A1515010925), Guangdong Provincial Key Laboratory of Information Photonics Technology (2020B121201011), Shenzhen Science and Technology Program (JCYJ20200109110608167), "One Hundred Talents Program" of the Guangdong University of Technology (GDUT) (1108-

220413205), the Open Fund of Guangdong Provincial Key Laboratory of Luminescence from Molecular Aggregates, Guangzhou 510640, China (South China University of Technology) (2019B030301003), Science and Technology Planning Project of Hunan Province (2018TP1017), CR thanks the University of Hull for support. XF would like to thank Analysis and Test Center of Guangdong University of technology for HRMS measurement.

REFERENCES

(1) Huang, Y.; Chen, W.; Chung, J.; Yin, J.; Yoon, J. Recent progress in fluorescent probes for bacteria. *Chem. Soc. Rev.* **2021**, *50*, 7725-7744.
(2) Prajapati, J. D.; Kleinekathofer, U.; Winterhalter, M. How to Enter a Bacterium: Bacterial Porins and the Permeation of Antibiotics. *Chem. Rev.* **2021**, *121*, 5158-5192.
(3) Klebba, P. E.; Newton, S. M. C.; Six, D. A.; Kumar, A.; Yang, T.; Nairn, B. L.; Munger, C.; Chakravorty, S. Iron Acquisition Systems of Gram-negative Bacterial Pathogens Define TonB-Dependent Pathways to Novel Antibiotics. *Chem. Rev.* **2021**, *121*, 5193-5239.
(4) Chen, W.; Li, Q.; Zheng, W.; Hu, F.; Zhang, G.; Wang, Z.; Zhang, D.; Jiang, X. Identification of bacteria in water by a fluorescent array. *Angew. Chem. Int. Ed.* **2014**, *53*, 13734-13739.
(5) Acharya, Y.; Bhattacharyya, S.; Dhanda, G.; Haldar, J. Emerging Roles of Glycopeptide Antibiotics: Moving beyond Gram-Positive Bacteria. *ACS. Infect. Dis.* **2022**, *8*, 1-28.
(6) Pandeya, A.; Ojo, I.; Alegun, O.; Wei, Y. Periplasmic Targets for the Development of Effective Antimicrobials against Gram-Negative Bacteria. *ACS. Infect. Dis.* **2020**, *6*, 2337-2354.
(7) Liu, X.; Qi, G.; Wu, M.; Pan, Y.; Liu, B. Universal Fluorescence Light-Up Gram-Staining Technique for Living Bacterial Differentiation. *Chem. Mater.* **2021**, *33*, 9213-9220.
(8) Wang, D.; Tang, B. Z. Aggregation-Induced Emission Luminogens for Activity-Based Sensing. *Acc. Chem. Res.* **2019**, *52*, 2559-2570.
(9) Zhang, Q.; Yu, P.; Fan, Y.; Sun, C.; He, H.; Liu, X.; Lu, L.; Zhao, M.; Zhang, H.; Zhang, F. Bright and Stable NIR-II J-Aggregated AIE Dibodipy-Based Fluorescent Probe for Dynamic In Vivo Bioimaging. *Angew. Chem. Int. Ed.* **2021**, *60*, 3967-3973.
(10) Mei, J.; Leung, N. L. C.; Kwok, R. T. K.; Lam, J. W. Y.; Tang, B. Z. Aggregation-Induced Emission: Together We Shine, United We Soar! *Chem. Rev.* **2015**, *115*, 11718-11940.
(11) Leung, C. W.; Hong, Y.; Chen, S.; Zhao, E.; Lam, J. W.; Tang, B. Z. A photostable AIE luminogen for specific mitochondrial imaging and tracking. *J. Am. Chem. Soc.* **2013**, *135*, 62-65.
(12) Larsen, L. G.; Crimaldi, J. P. The effect of photobleaching on PLIF. *Exp. Fluids* **2006**, *41*, 803-812.
(13) Luo, J.; Xie, Z.; Lam, J. W.; Cheng, L.; Chen, H.; Qiu, C.; Kwok, H. S.; Zhan, X.; Liu, Y.; Zhu, D.; Tang, B. Z. Aggregation-induced emission of 1-methyl-1,2,3,4,5-pentaphenylsilole. *Chem. Commun.* **2001**, 1740-1741.
(14) Hu, R.; Zhou, F.; Zhou, T.; Shen, J.; Wang, Z.; Zhao, Z.; Qin, A.; Tang, B. Z. Specific discrimination of gram-positive bacteria and direct visualization of its infection towards mammalian cells by a DPAN-based AIEgen. *Biomaterials* **2018**, *187*, 47-54.
(15) Ji, C.; Lai, L.; Li, P.; Wu, Z.; Cheng, W.; Yin, M. Organic dye assemblies with aggregation‐induced photophysical changes and their bio‐applications. *Aggregate* **2021**, *2*, e39.
(16) Xu, W.; Wang, D.; Tang, B. Z. NIR-II AIEgens: A Win-Win Integration towards Bioapplications. *Angew. Chem. Int. Ed.* **2021**, *60*, 7476-7487.
(17) Feng, X.; Li, Y.; He, X. ; Liu, H.; Zhao, Z.; Kwok, R. T. K.; Elsegood, M. R. J.; Lam, J. W. Y.; Tang, B. Z. A Substitution-Dependent Light-Up Fluorescence Probe for Selectively Detecting Fe^{3+} Ions and Its Cell Imaging Application. *Adv. Funct. Mater.* **2018**, *28*, 1802833.
(18) Zhang, R.; Huang, X.; Chen, C.; Kwok, R. T. K.; Lam, J. W. Y.; Tang, B. Z. AIEgen for cancer discrimination. *Mater. Sci. Eng. R Rep.* **2021**, *146*. 100649.
(19) Chen, J.; Feng, S.; Chen, M.; Li, P.; Yang, Y.; Zhang, J.; Xu, X.; Li, Y.; Chen, S. In Vivo Dynamic Monitoring of Bacterial Infection by NIR-II Fluorescence Imaging. *Small* **2020**, *16*, e2002054.
(20) Li, J.; Meng, Z.; Zhuang, Z.; Wang, B.; Dai, J.; Feng, G.; Lou, X.; Xia, F.; Zhao, Z.; Tang, B. Z. Effective Therapy of Drug-Resistant Bacterial Infection by Killing Planktonic Bacteria and Destructing Biofilms with Cationic Photosensitizer Based on Phosphindole Oxide. *Small* **2022**, *18*, e2200743.
(21) Yoon, J. Turning an FDA‐approved therapeutic into an AIEgen for imaging live bacteria and for bacterial detection. *Aggregate* **2021**, *2*, e47.
(22) Liu, G.; Tian, S.; Li, C. ; Xing, G. ; Zhou, L. Aggregation-Induced-Emission Materials with Different Electric Charges as an Artificial Tongue: Design, Construction, and Assembly with Various Pathogenic Bacteria for Effective Bacterial Imaging and Discrimination. *ACS Appl. Mater. Interfaces* **2017**, *9*, 28331-28338.
(23) Zhao, E.; Hong, Y.; Chen, S.; Leung, C. W.; Chan, C. Y.; Kwok, R. T.; Lam, J. W.; Tang, B. Z. Highly fluorescent and photostable probe for long-term bacterial viability assay based on aggregation-induced emission. *Adv. Healthc Mater.* **2014**, *3*, 88-96.
(24) Shi, X.; Sung, S. H. P.; Chau, J. H. C.; Li, Y.; Liu, Z.; Kwok, R. T. K.; Liu, J.; Xiao, P.; Zhang, J.; Liu, B.; Lam, J. W.; Tang, B. Z. Killing G(+) or G(−) Bacteria? The Important Role of Molecular Charge in AIE‐Active Photosensitizers. *Small Methods* **2020**, *4*, 2000046.
(25) Zhou, C.; Jiang, M.; Du, J.; Bai, H.; Shan, G.; Kwok, R. T. K.; Chau, J. H. C.; Zhang, J.; Lam, J. W. Y.; Huang, P.; Tang, B. Z. One stone, three birds: one AIEgen with three colors for fast differentiation of three pathogens. *Chem. Sci.* **2020**, *11*, 4730-4740.
(26) Liang, J.; Tang, B. Z.; Liu, B. Specific light-up bioprobes based on AIEgen conjugates. *Chem. Soc. Rev.* **2015**, *44*, 2798-2811.
(27) Li, L.; Chen, L.; Lu, Y.; Li, B.; Hu, R.; Huang, L.; Zhang, T.; Wei, X.; Yang, Z.; Mao, C. Aggregated carbon dots‐loaded macrophages treat sepsis by eliminating multidrug‐resistant bacteria and attenuating inflammation. *Aggregate* **2022**. DOI: 10.1002/agt2.200.
(28) Chen, K.; He, P.; Wang, Z.; Tang, B. Z. A Feasible Strategy of Fabricating Type I Photosensitizer for Photodynamic Therapy in Cancer Cells and Pathogens. *ACS Nano* **2021**, *15*, 7735-7743.
(29) Feng, G.; Yuan, Y.; Fang, H.; Zhang, R.; Xing, B.; Zhang, G.; Zhang, D.; Liu, B. A light-up probe with aggregation-induced emission characteristics (AIE) for selective imaging, naked-eye detection and photodynamic killing of Gram-positive bacteria. *Chem. Commun.* **2015**, *51*, 12490-12493.
(30) Gong, J.; Han, J.; Liu, Q.; Ren, X.; Wei, P.; Yang, L.; Zhang, Y.; Liu, J.; Dong, Y.; Wang, Y.; Song, X.; Tang, B. Z. An ideal platform of light-emitting materials from phenothiazine: facile preparation, tunable red/NIR fluorescence, bent geometry-promoted AIE behaviour and selective lipid-droplet (LD) tracking ability. *J. Mater. Chem. C* **2019**, *7*, 4185-4190.
(31) Hauck, M.; Stolte, M.; Schonhaber, J.; Kuball, H. G.; Muller, T. J. Synthesis, electronic, and electro-optical properties of emissive solvatochromic phenothiazinyl merocyanine dyes. *Chem. Eur. J* **2011**, *17*, 9984-9998.
(32) Mao, X.; Xie, F.; Wang, X.; Wang, Q.; Qiu, Z.; Elsegood, M. R. J.; Bai, J.; Feng, X.; Redshaw, C.; Huo, Y.; Hu, J.-Y.; Chen, Q. New Quinoxaline‐Based Blue Emitters: Molecular Structures, Aggregation‐Induced Enhanced Emission Characteristics and OLED Application. *Chin. J. Chem.* **2021**, *39*, 2154-2162.
(33) Gao, M.; Su, H.; Li, S.; Lin, Y.; Ling, X.; Qin, A.; Tang, B. Z. An easily accessible aggregation-induced emission probe for lipid droplet-specific imaging and movement tracking. *Chem. Commun.* **2017**, *53*, 921-924.
(34) Horobin, R. W.; Rashid-Doubell, F.; Pediani, J. D.; Milligan, G. Predicting small molecule fluorescent probe localization in living cells using QSAR modeling. 1. Overview and models for probes of structure, properties and function in single cells. *Biotech. Histochem.* **2013**, *88*, 440-460.
(35) Yin, W.; Li, Y.; Li, N.; Yang, W.; An, H.; Gao, J.; Bi, Y.; Zhao, N. Hybridization of Triphenylamine and Salicylaldehyde: A Facile Strategy to Construct Aggregation‐Induced Emission Luminogens with Excited‐State Intramolecular Proton Transfer for Specific Lipid Droplets and Gram‐Positive Bacteria Imaging. *Adv. Opt. Mater.* **2020**, *8*, 1902027.
(36) Niu, G.; Zhang, R.; Kwong, J. P. C.; Lam, J. W. Y.; Chen, C.; Wang, J.; Chen, Y.; Feng, X.; Kwok, R. T. K.; Sung, H. H. Y.; Williams, I. D.; Elsegood, M. R. J. Qu, J.; Ma, C.; Wong, K. S.; Yu, X.; Tang, B. Z. Specific Two-Photon Imaging of Live Cellular and Deep-Tissue Lipid Droplets by Lipophilic AIEgens at Ultralow Concentration. *Chem. Mater.* **2018**, *30*, 4778-4787.
(37) Li, Y.; Zhao, Z.; Zhang, J. ; Kwok, R. T. K.; Xie, S.; Tang, R. ; Jia, Y. ; Yang, J. ; Wang, L.; Lam, J. W. Y.; Zheng, W.; Jiang, X.; Tang, B. Z. A Bifunctional Aggregation-Induced Emission Luminogen for Monitoring and Killing of Multidrug-Resistant Bacteria. *Adv. Funct. Mater.* **2018**, *28*, 1804632.

(38) Cai, X.; Xie, N.; Li, Y.; Lam, J. W. Y.; Liu, J.; He, W.; Wang, J.; Tang, B. Z. A smart AIEgen-functionalized surface with reversible modulation of fluorescence and wettability. *Mater. Horiz.* **2019**, *6*, 2032-2039.
(39) Borjihan, Q.; Wu, H.; Dong, A.; Gao, H.; Yang, Y. W. AIEgens for Bacterial Imaging and Ablation. *Adv. Healthc Mater.* **2021**, *10*, e2100877.
(40) Lee, M. M. S.; Yan, D.; Chau, J. H. C.; Park, H.; Ma, C. C. H.; Kwok, R. T. K.; Lam, J. W. Y.; Wang, D.; Tang, B. Z. Highly efficient phototheranostics of macrophage-engulfed Gram-positive bacteria using a NIR luminogen with aggregation-induced emission characteristics. *Biomaterials* **2020**, *261*, 120340.
(41) Soh, N. Recent advances in fluorescent probes for the detection of reactive oxygen species. *Anal. Bioanal. Chem.* **2006**, *386*, 532-543.
(42) Sohlenkamp, C.; Geiger, O. Bacterial membrane lipids: diversity in structures and pathways. *FEMS Microbiol. Rev.* **2016**, *40*, 133-159.
(43) Tsuchiya, M.; Tamura, T.; Hamachi, I. Organelle-Selective Labeling of Choline-Containing Phospholipids (CPLs) and Real-Time Imaging in Living Cells. *Curr. Protoc.* **2021**, *1*, e105.
(44) Greening, C.; Lithgow, T., Formation and function of bacterial organelles. *Nat. Rev. Microbiol.* **2020,** *18*, 677-689.
(45) Kang, M.; Zhou, C.; Wu, S.; Yu, B.; Zhang, Z.; Song, N.; Lee, M. M. S.; Xu, W.; Xu, F. J.; Wang, D.; Wang, L.; Tang, B. Z., Evaluation of Structure-Function Relationships of Aggregation-Induced Emission Luminogens for Simultaneous Dual Applications of Specific Discrimination and Efficient Photodynamic Killing of Gram-Positive Bacteria. *J. Am. Chem. Soc.* **2019**, *141*, 16781-16789.
(46) Li, Y.; Liu, F.; Zhang, J.; Liu, X.; Xiao, P.; Bai, H.; Chen, S.; Wang, D.; Sung, S. H. P.; Kwok, R. T. K.; Shen, J.; Zhu, K.; Tang, B. Z., Efficient Killing of Multidrug-Resistant Internalized Bacteria by AIEgens In Vivo. *Adv. Sci.* **2021**, *8*, 2001750.
(47) Wang, B.; Yu, J.; Sui, L.; Zhu, S.; Tang, Z.; Yang, B.; Lu, S., Rational Design of Multi-Color-Emissive Carbon Dots in a Single Reaction System by Hydrothermal. *Adv. Sci.* **2020**, *8*, 2001453.
(48) Dias, C.; Pais, J. P.; Nunes, R.; Blazquez-Sanchez, M. T.; Marques, J. T.; Almeida, A. F.; Serra, P.; Xavier, N. M.; Vila-Vicosa, D.; Machuqueiro, M.; Viana, A. S.; Martins, A.; Santos, M. S.; Pelerito, A.; Dias, R.; Tenreiro, R.; Oliveira, M. C.; Contino, M.; Colabufo, N. A.; de Almeida, R. F. M.; Rauter, A. P., Sugar-based bactericides targeting phosphatidylethanolamine- enriched membranes. *Nat. Commun.* **2018**, *9*. 4857.
(49) Whitfield, C.; Trent, M. S., Biosynthesis and export of bacterial lipopolysaccharides. *Annu. Rev. Biochem.* **2014,** *83*, 99-128.
(50) Boll, J. M.; Crofts, A. A.; Peters, K.; Cattoir, V.; Vollmer, W.; Davies, B. W.; Trent, M. S., A penicillin-binding protein inhibits selection of colistin-resistant, lipooligosaccharide-deficient Acinetobacter baumannii. *Proc. Natl. Acad. Sci. USA* **2016,** *113*, E6228-E6237.

Table of Contents.

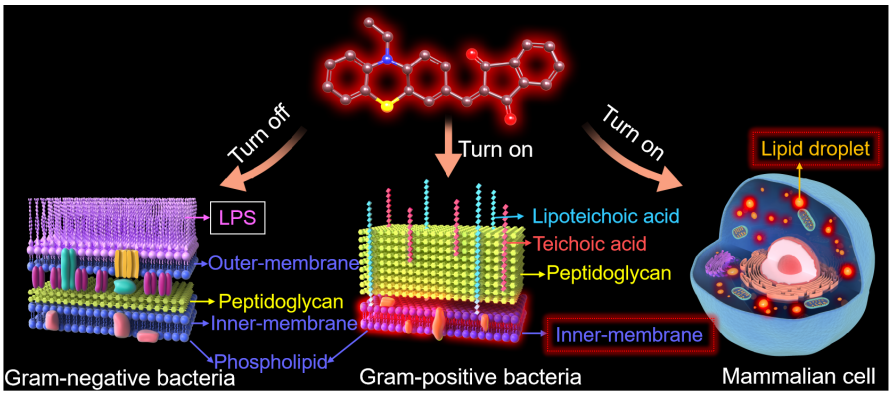

We present an electrically neutral, red fluorophore with aggregation-induced enhanced emission (AIEE) characteristics, which can not only stain lipid droplets in mammalian cells, but also specifically differentiate G+ and G- bacteria.
